Ecotoxicology and Environmental Safety 214 (2021) 112113

Contents lists available at ScienceDirect

Ecotoxicology and Environmental Safety

journal homepage: www.elsevier.com/locate/ecoenv

Laser-induced breakdown spectroscopy as a straightforward bioimaging tool for plant biologists; the case study for assessment of photon-upconversion nanoparticles in *Brassica oleracea* L. plant

Pavlína Modlitbová [a], Sára Střítežská [a], Antonín Hlaváček [b], David Prochazka [a,c], Pavel Pořízka [a,c,*], Jozef Kaiser [a,c]

[a] Central European Institute of Technology (CEITEC) Brno University of Technology, Purkyňova 123, 612 00 Brno, Czech Republic
[b] Institute of Analytical Chemistry of the Czech Academy of Sciences, Veveří 97, 602 00 Brno, Czech Republic
[c] Faculty of Mechanical Engineering, Brno University of Technology, Technická 2896/2, 616 69 Brno, Czech Republic

ARTICLE INFO

Edited by Dr G Liu

Keywords:
Rare-earth elements
Yttrium
Ytterbium
Thulium
Cabbage
LIBS
Spatial element distribution
Translocation
Bioaccumulation

ABSTRACT

The main purpose of this work is to thoroughly describe the implementation protocol of laser-induced breakdown spectroscopy (LIBS) method in the plant analysis. Numerous feasibility studies and recent progress in instrumentation and trends in chemical analysis make LIBS an established method in plant bioimaging. In this work, we present an easy and straightforward phytotoxicity case study with a focus on LIBS method. We intend to demonstrate in detail how to manipulate with plants after exposures and how to prepare them for analyses. Moreover, we aim to achieve 2D maps of spatial element distribution with a good resolution without any loss of sensitivity. The benefits of rapid, low-cost bioimaging are highlighted.

In this study, cabbage (*Brassica oleracea* L.) was treated with an aqueous dispersion of photon-upconversion nanoparticles ($NaYF_4$ doped with Yb^{3+} and Tm^{3+} coated with carboxylated silica shell) in a hydroponic short-term toxicity test. After a 72-hour plant exposure, several macroscopic toxicity end-points were monitored. The translocation of Y, Yb, and Tm across the whole plant was set by employing LIBS with a lateral resolution 100 μm. The LIBS maps of rare-earth elements in *B.oleracea* plant grown with 50 μg/mL nanoparticle-treated and ion-treated exposures showed the root as the main storage, while the transfer *via* stem into leaves was minimal. On the contrary, the LIBS maps of plants exposed to the 500 μg/mL nanoparticle-treated and ion-treated uncover slightly different trends, nanoparticles as well as ions were transferred through the stem into leaves. However, the main storage organ was a root as well.

1. Introduction

Many types of nanoparticles (NPs) have been increasingly used in commercial products as well as in many research areas. This leads not only to the NP-accumulation in the environment and within the food chain (Rodrigues et al., 2016) but also to unknown toxic effects at various organism/tissue/cellular levels (Magnuson et al., 2011). The evaluation of NPs toxicity, bioaccumulation, and translocation in diverse organisms is an extremely challenging task (Modlitbová et al., 2020a). This is caused by a great number of variables in physicochemical properties of NPs (composition, shape, size, surface charge, functional group and ligands, …). Thus, it is impossible to establish robust standard protocols. Consequently, the real effects of NPs and the sites of their bioaccumulation still remain unknown.

The precise localization of NPs through the plant tissues is of a paramount importance in order to reveal the relationship between the exact location of NPs and their toxic effect. The distribution of NPs and their bioimaging in plants is evaluated most often by using transmission electron microscopy (Wang et al., 2012), scanning electron microscopy (Vittori Antisari et al., 2015), scanning transmission electron microscopy (Schwabe et al., 2015), micro-X-ray fluorescence microscopy (Cui et al., 2014), or laser ablation inductively coupled plasma mass spectrometry (Ko et al., 2019). However, rarely has been laser-induced breakdown spectroscopy (LIBS) showed to be suitable for a spatial distribution of elements contained in NPs assessment within various plant organs in a few recent papers (Krajcarová et al., 2017; Modlitbová et al.,

* Corresponding author at: Central European Institute of Technology (CEITEC) Brno University of Technology, Purkyňova 123, 612 00 Brno, Czech Republic.
E-mail address: pavel.porizka@ceitec.vutbr.cz (P. Pořízka).

https://doi.org/10.1016/j.ecoenv.2021.112113
Received 14 December 2020; Received in revised form 17 February 2021; Accepted 26 February 2021
Available online 6 March 2021

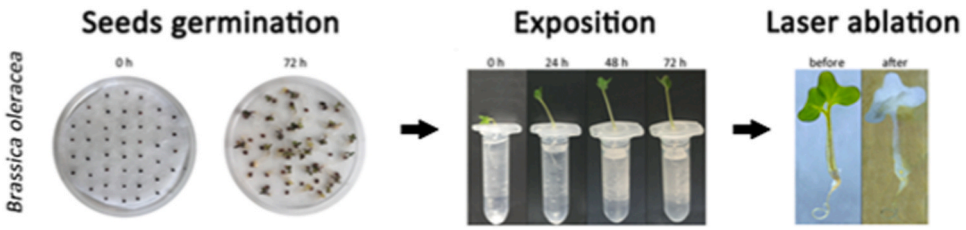

Fig. 1. Scheme of seeds germination, plant exposure, and plant samples before and after LIBS analysis.

2019, 2020b). Herein, LIBS represents an indispensable alternative to its analytical counterparts in the NPs bioimaging with a high resolution (micro-scale) on a large-scale sample (whole glass slide imaging).

The LIBS has been widely used in modern analytical chemistry. It is popular because of its advantages such as the fast turn-around time, multi-elemental capability (detection of light elements and halogens), analysis of samples in any state of matter, possibility of remote sensing, and the assessment of spatial elemental distribution on a large scale (so called imaging). Various biological samples were successfully analysed using LIBS method, e.g., mouse kidney, lung tumours, skin melanomas; summarized in two most recent reviews (Busser et al., 2018; Jolivet et al., 2019). LIBS was also applied for bioimaging of various NP types in plant tissues as mentioned above (Modlitbová et al., 2020a).

In this study, less common NPs, the rare-earth elements-doped photon-upconversion nanoparticles (UCNPs) are studied. The UCNPs are a new type of luminescent nanomaterial which started to be widely used as luminescent labels due to their unique optical properties (Zhou et al., 2015). They are composed of $NaYF_4$ nanocrystals and doped with Yb^{3+} and Tm^{3+} ions; a carboxylated silica shell is added on the surface to increase the chemical stability and reduce the releasing of free ions (Modlitbová et al., 2019).

The cabbage (*Brassica oleracea* L.), which has been commonly used as a model crop plant in phytotoxicity and bioaccumulation experiments tests for a long time (Wang and Keturi, 1990), was employed during the whole study. This plant species belongs to ten recommended species by United States Environmental Protection Agency (US EPA) for the determination of toxicological effects of pesticides and other toxic substances (US EPA, 1996). Additionally, the cabbage belongs to the so-called hyperaccumulator plant family Brassicaceae (Reeves et al., 2018). Also, this plant was already used in the phytotoxicity assessment of various NPs, for example Ag NPs (Pokhrel and Dubey, 2013), ZnO NPs (Pokhrel and Dubey, 2013), Al_2O_3 NPs (Amist et al., 2017), and CuO NPs (Singh et al., 2017). Moreover, the phytotoxicity of rare-earth elements containing NPs (CeO_2, La_2O_3, Gd_2O_3, and Yb_2O_3 NPs) was established and the growth of cabbage root was negatively affected by La_2O_3, Gd_2O_3, and Yb_2O_3 NPs dispersions in a very high test concentration 2000 μg NPs/mL (Ma et al., 2010).

In this study, the first objective was to evaluate the toxicity of the selected contaminants (UCNPs dispersion in two nominal concentrations 500 and 50 μg UCNPs/mL, and two Y^{3+} and Yb^{3+} mixture solutions in corresponding concentrations serving as a positive control) to *B. oleracea* plant grow in an aqueous medium. After a 72-h exposure, we monitored four macroscopic end-points (root length, stem length, root + stem length, whole plant length). Then, the spatial distribution of Y, Yb, and Tm for UCNPs treated plants, and the spatial distribution of Y and Yb for positive control treated plants was set by LIBS method. The photon-upconversion laser microscanning was used as a complementary technique confirming the presence of Y, Yb, and Tm in the plants in the form of UCNPs (Sedlmeier et al., 2016).

The spatial distribution of Y, Yb (Tm) across the whole plant was established with a sufficient spatial resolution of 100 μm by LIBS. The difference in behaviour between both contaminants as well as between both tested concentrations is clearly visible in obtained 2D maps. LIBS is a fast, straightforward, price sensitive (when compared to Laser Ablation Inductively Coupled Plasma Mass Spectrometry), and relatively simple analytical method for semi-quantitative multi-element bioimaging in plants with a similar sensitivity to the photon-upconversion microscanner. Moreover, LIBS is a promising alternative to other techniques as it is able to detect NPs with no visible upconversion or fluorescence. It also detects NPs whose luminescence is quenched, e.g. because of changes in external conditions, such as pH values changes (Škarková et al., 2017).

2. Material and methods

2.1. Synthesis and characterization of UCNPs

The preparation of UCNPs was described in detail in our previous work (Hlaváček et al., 2019), nothing was modified in this experiment. These were the used reagents: $YCl_3 \times 6H_2O$ (99.99%), $YbCl_3 \times 6H_2O$ (99.99%), $TmCl_3 \times 6H_2O$ (99.99%), 1-octadecene (90%), oleic acid (90%), tetraethylorthosilicate (TEOS, ≥ 99%), and Igepal CO-520 were purchased from Sigma-Aldrich (Steinheim, Germany) and used as starting materials without further purification. NaOH (p.a.), cyclohexane (p.a.), N,N-Dimethylformamide (p.a.), Methanol (p.a.), Acetone (p.a.), and NH_4OH 25% (p.a.) were purchased from PENTA (Chrudim, Czech Republic). Carboxyethylsilanetriol, sodium salt; 25% (w/v) in water was obtained from ABCR GmbH (Karlsruhe, Germany). The nominal hydrodynamic particle diameter was determined with a Zetasizer Nano ZS (Malvern Instruments, Worcestershire, United Kingdom).

2.2. Plant exposure

Seeds of cabbage (*Brassica oleracea* L.) were purchased from MoravoSeed (Mikulov, Czech Republic). Firstly, cabbage seeds were germinated for 48 h in Petri dishes with the bottom covered with filtration paper in Milli-Q water (Millipore RG, Merck KGaA, Germany). Then seedlings with similar size (approximately 1 cm root length) were selected for the toxicity test. Plants were exposed for 72 h under the lighting cycle of 15 h light/9 h darkness at room temperature (22 ± 1 °C). Specially prepared Eppendorf tubes with a 2-mm hole on the top were filled with 2.0 mL of an exposure medium based on our previous studies (Modlitbová et al., 2020b). Each plant experiment consisted of a control group (Milli-Q water), two UCNPs dispersions in nominal concentrations 500 μg UCNPs/mL (100 μg Y/mL + 43.8 μg Yb/mL) and 50 μg UCNPs/mL (10 μg Y/mL + 4.38 μg Yb/mL), and two chloride mixture solutions at the same concentrations "500″ μg /mL (100 μg Y/mL + 43.8 μg Yb/mL) and "50″ μg/mL (10 μg Y/mL + 4.38 μg Yb/mL). Each exposure group contained 12 replicates of test plants. After the 72-hour exposure, the plants were photographed; plant roots, stems, and the overall length were measured. A simplified scheme of toxicity test followed by LIBS measurements is illustrated in Fig. 1.

The statistical analysis for root, stem, root + stem, and the whole plant length (5–11 plants per one treatment) was performed by OriginPro software (2015). The significance of the difference between the exposed and control plants was tested by the Mann-Whitney *U*-test. The level of significance was accepted at $^{*}p < 0.05$, $^{**}p < 0.01$, and $^{***}p < 0.001$.

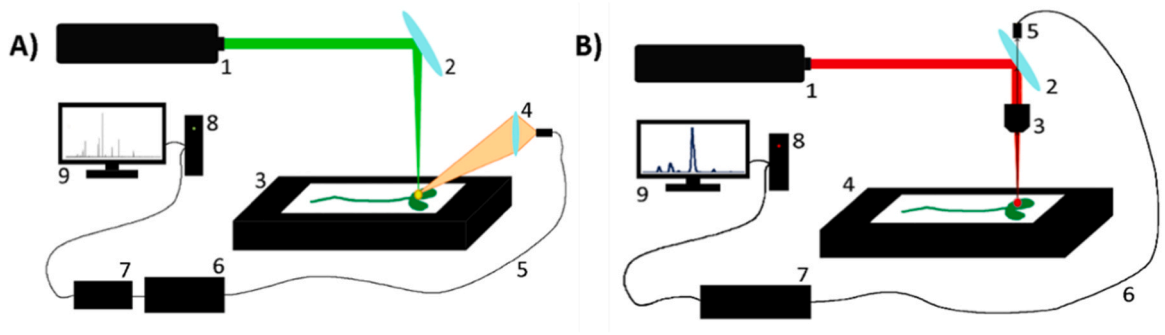

Fig. 2. A) LIBS scheme: (1) laser, (2) focusing optics, (3) sample holder with plant sample, (4) collection optics, (5) optical fibre, (6) spectrometer, (7) detector, (8) PC, (9) example of LIBS emission spectra. 2B) Laser microscanner scheme: (1) laser and focusing optics, (2) dichroic mirror, (3) microscope objective, (4) sample holder with plant sample, (5) collection optics, (6) optical fiber, (7) spectrometer, (8) PC, (9) example of photon-upconversion spectra.

2.3. LIBS bioimaging

After the exposure, plants must be prepared for LIBS measurements (Jantzi et al., 2016). Several ways to prepare plants were already and summarized in an extensive review (Modlitbová et al., 2020a). These approaches are the most common. The first way is to use fresh plants and analyze them directly, even in *in-situ* conditions (Zhao et al., 2016). The main disadvantage is the water content in plants which is responsible for lower LIBS signals (Peng et al., 2017), and for no possibility of the experiment repetition. The second procedure is to prepare histological cross-sections from plant tissues (Krajcarová et al., 2017). This is a very time consuming procedure which requires a detailed optimalization for various plant tissues, different contaminants as well as for different laser sources in LIBS set-ups. The third possibility is the most common, easy, and low-cost. It was used in this experiment. The plants were firstly thoroughly washed in Milli-Q water, then dried and molded at room temperature for five days and then glued with epoxide onto the glass slide. Then, plants were photographed using an optical microscope (Stemi 2000-c, Zeiss, Oberkochen, Germany), then photon-upconversion microscans (only in case of UCNPs treated plants), and LIBS measurements were performed.

The LIBS Discovery system (CEITEC, Brno, Czech Republic) was used for all experiments. The set-up consisted of a nanosecond laser (CFR 400, Quantel, Paris, France; 20 Hz, 532 nm, 10 ns), UV grade collecting optic (F2, SOL instruments, Minsk, Belarus), an optical fibre (core diameter 400 μm, Thorlabs, Newton, United States), the glass doublet (f = 32 mm, Sill optics, Wendelstein, Germany), the Czerny-Turner spectrometer (Shamrock, Andor, Nottingham, United Kingdom), and a sCMOS iStar camera (Andor). A simplified scheme of LIBS experiment set-up is illustrated in Fig. 2A.

The experimental parameters used during the LIBS analysis were optimized in our previous work (Modlitbová et al., 2019) and only slight

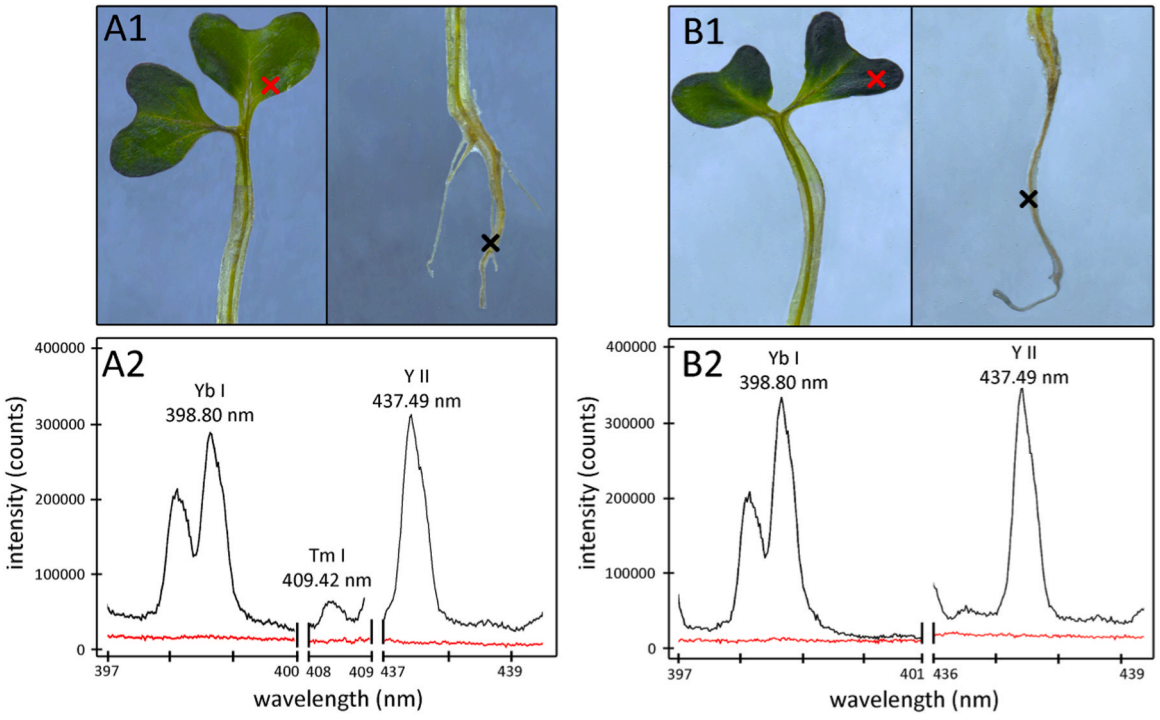

Fig. 3. A1) The photograph of plant treated with UCNPs dispersion (leaves – left side, root – right side). The black cross represents place with UCNPs contain and the red cross represents places without UCNPs contain. Followingly typical LIBS spectrum (black – with UCNPs presence, red – without UCNPs presence) with marked emission lines are at part A2. B1) The photograph of the plant treated with ions solution (leaves – left side, root – right side). The black cross represents place with the Y and Yb contain and the red cross represents places without the Y and Yb contain. Followingly typical LIBS spectrum (black – with Y and Yb presence, red – without Y and Yb presence) with marked emission lines are at part B2. (For interpretation of the references to colour in this figure legend, the reader is referred to the web version of this article.)

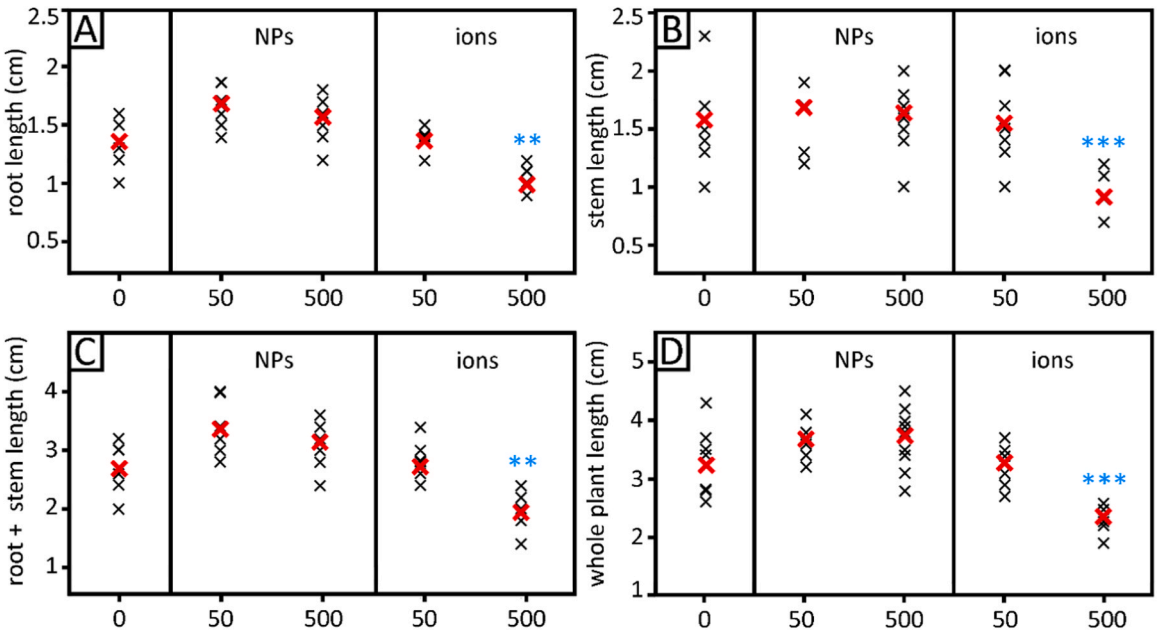

Fig. 4. Toxicological macroscopic end-points for cabbage (B. oleracea) after a 72 h exposure to UCNPs dispersions and ions mixture solutions, the x axis shows nominal concentrations (μg/mL), each black cross represents one sample and each red cross is a mean, the blue asterisks show notable differences (*$p < 0.05$, **$p < 0.01$, ***$p < 0.001$), A: root length (cm), B: stem length (cm), C: root + stem length (cm), D: length of the whole plant (cm). (For interpretation of the references to colour in this figure legend, the reader is referred to the web version of this article.)

modifications were made here. The 1 μs of the gate delay, 15 μs of the detection integration time, 20 mJ of laser pulse energy, and 20 Hz repetition rate were preserved. The energy per pulse and number of ablation layers needed for the whole plant mass removing have to be optimized again due to a different plant structure of each test plant species. The energy was set to 20 mJ per pulse which was enough for ablation of the whole plant mass in one layer. The irradiance value was approximately 6.3 GW cm^{-2}. The lateral resolution was 100 μm based on the crater diameter. The resolution of maps is already a compromise between the laser beam energy, the size of crater diameter after the laser ablation, and the achieved sensitivity. The typical map size ranged from 150 to 400 mm^2 and consisted from 20,382 to 40,584 spectra; the measurements times were between 17 and 34 min.

The data from LIBS measurements of plant samples were analysed using RStudio (R-Core team, Vienna, Austria), LIBS Analyzer (CEITEC, Brno, Czech Republic), and Lightigo ImageLab (Epina, Vienna, Austria). The most appropriate emission lines were Y II 437.49 nm, Yb I 398.80 nm, and Tm I 409.42 nm. These lines were selected based on literature (Modlitbová et al., 2019). Afterwards, they were experimentally verified, i.e. 100 spectra were obtained from solid Y_2O_3 (p.a., Lachema, Brno, Czech Republic), Yb_2O_3 (p.a., Ubichem, Redditch, United Kingdom), and Tm_2O_3 (p.a., Sigma Aldrich) standards. Spectra of selected elements were thoroughly investigated and spectral lines assigned. For those purposes we have also used Principal Component Analysis (PCA), all the spectra were processed using PCA and yielded loadings showed distinct spectral lines for individual elements (Pořízka et al., 2018). These lines were used through the whole experiment after a background subtraction using moving minimum (Yaroshchyk and Eberhardt, 2014) where the size of the minimum window was set at 80 points and the smoothing window at 30 points. The data were imaged in the form of 2D maps. Each point of the map represents one obtained spectrum, thus it gives the spatial resolution. The intensity is represented by the integral of the area under the spectral line. Fig. 3 depicts the obtained spectra from plants treated with UCNPs dispersions as well as with ions mixture.

2.4. Photon-upconversion microscans

Plants exposed to UCNPs dispersions were scanned with a photon-upconversion microscanner before LIBS measurements. A laser diode (5 W, 976 nm, Besram Technology, Wuhan, China) with a focusing lens (focal length 20 mm, ThorLabs) and a 925 nm long-pass filter (Edmund Optics, Barrington, United States) was utilized as an excitation source for photon-upconversion luminescence. The detector of microscanner comprises a dichroic mirror (900 nm short pass, Thorlabs) that reflects the excitation into the microscope objective (40 ×, NA 0.60). The objective collects the luminescence into a charge-coupled device array spectroscope (QE65000, Ocean Optics, Duiven, the Netherlands) which is connected by a multimode optical fiber of 200 μm diameter (ThorLabs), and records emission spectra in the range from 435 nm to 900 nm. The spatial resolution of the scanner was set to 40 μm and the integration time of 10 ms was used for recording the emission spectrum in each pixel of the image. Recorded images confirmed the presence of UCNPs and evaluated the translocation of UCNPS through the root and stem to leaves. A simplified scheme of laser microscanner is shown in Fig. 2B.

3. Results and discussion

3.1. The properties of tested compounds

The photon-upconversion maximum and the hydrodynamic diameter of UCNPs in both concentrations was established before and after the exposures to *B. oleracea* (summarized in the Supplementary data file in Table S1). No evident changes before and after the exposure were noted in photon-upconversion maximum values, and only minimal changes were registered in the hydrodynamic diameter of NPs. This demonstrated a great stability of tested UCNPs with low tendencies to agglomerate/aggregate after a contact with the plant roots. Also, the nominal concentrations of Y, Yb, and Tm ions in UCNPs dispersions and positive control solutions are listed in the Supplementary data file in Table S2.

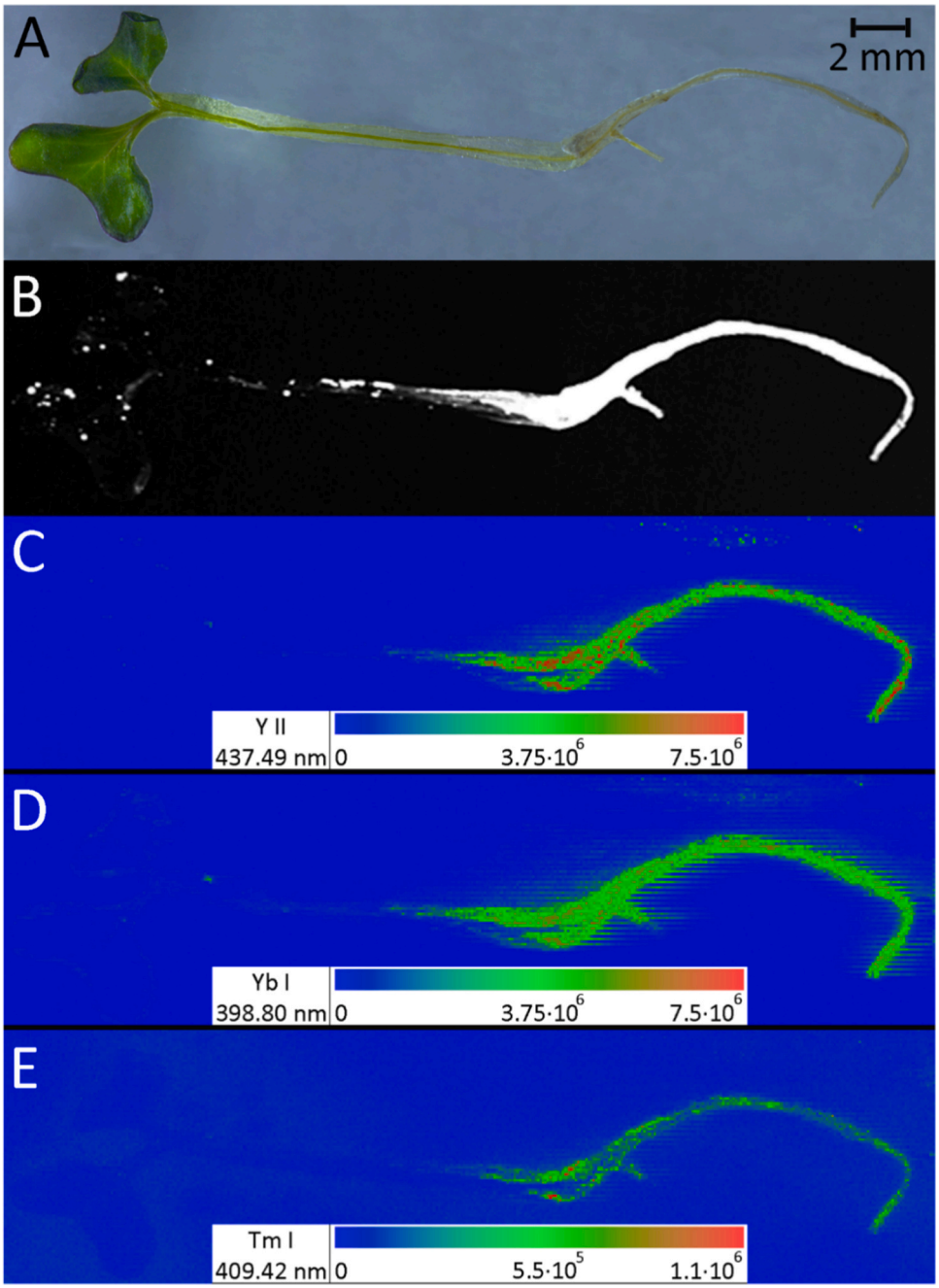

Fig. 5. Brassica oleracea after a 72-h exposure to 500 μg UCNPs/mL dispersion, A: photography of plant, B: photon-upconversion microscan of plant, C: 2D LIBS map of spatial yttrium distribution (Y II 437.49 nm), D: 2D LIBS map of spatial ytterbium distribution (Yb I 398.80 nm), E: 2D LIBS map of spatial thulium distribution (Tm I 409.42 nm). The scales show the intensity of emission lines (counts).

3.2. Toxicity experiments

The following parameters served as the macroscopic toxicity endpoints; the root length, stem length, root + stem length, and the whole plant length. Their significant affection was noticeable only in concentration "500″ μg/mL of ions mixture solution (100 μg Y/mL + 43.8 μg Yb/mL). The root length and root + stem length (Mann-Whitney *U* test, $^{**}p < 0.01$), and the stem and the whole plant length (Mann-Whitney *U* test, $^{***}p < 0.001$) were significantly negatively affected (Fig. 4). On the contrary, UCNPs dispersions in both tested concentrations (500 and 50 μg UCNPs/mL) had a slightly (not statistically significant) positive effect on the growth of all plant parts. The zero effect for all monitored parameters was noticed in concentration "50″ μg/mL of ions mixture solution (10 μg Y/mL + 4.38 μg Yb/mL).

The plant growth enhancement is expected in a low UCNPs exposure dosage. Concentration 10 μg UCNPs/mL promoted the development of mung beans (Peng et al., 2012), development of soybean (Yin et al., 2015), or the radish root growth (Modlitbová et al., 2019). Higher concentrations (100, 500, or 1000 μg UCNPs/mL) showed to have an inhibitory growth effect for exposed plants. In accordance with literature, the concentration 50 μg UCNPs/mL had no negative effect on *B. oleracea* growth. On the contrary to literature, *B. oleracea* growth was not inhibited even in the concentration 500 μg UCNPs/mL. This inconsistence could be partially affected by a slightly different type of tested UCNPs; $NaYF_4$:Yb^{3+},Er^{3+},Tm^{3+} coated with citric acid (Peng et al., 2012), $NaYF_4$:Yb^{3+},Er^{3+} coated with polyethyleneimine (Yin et al.,

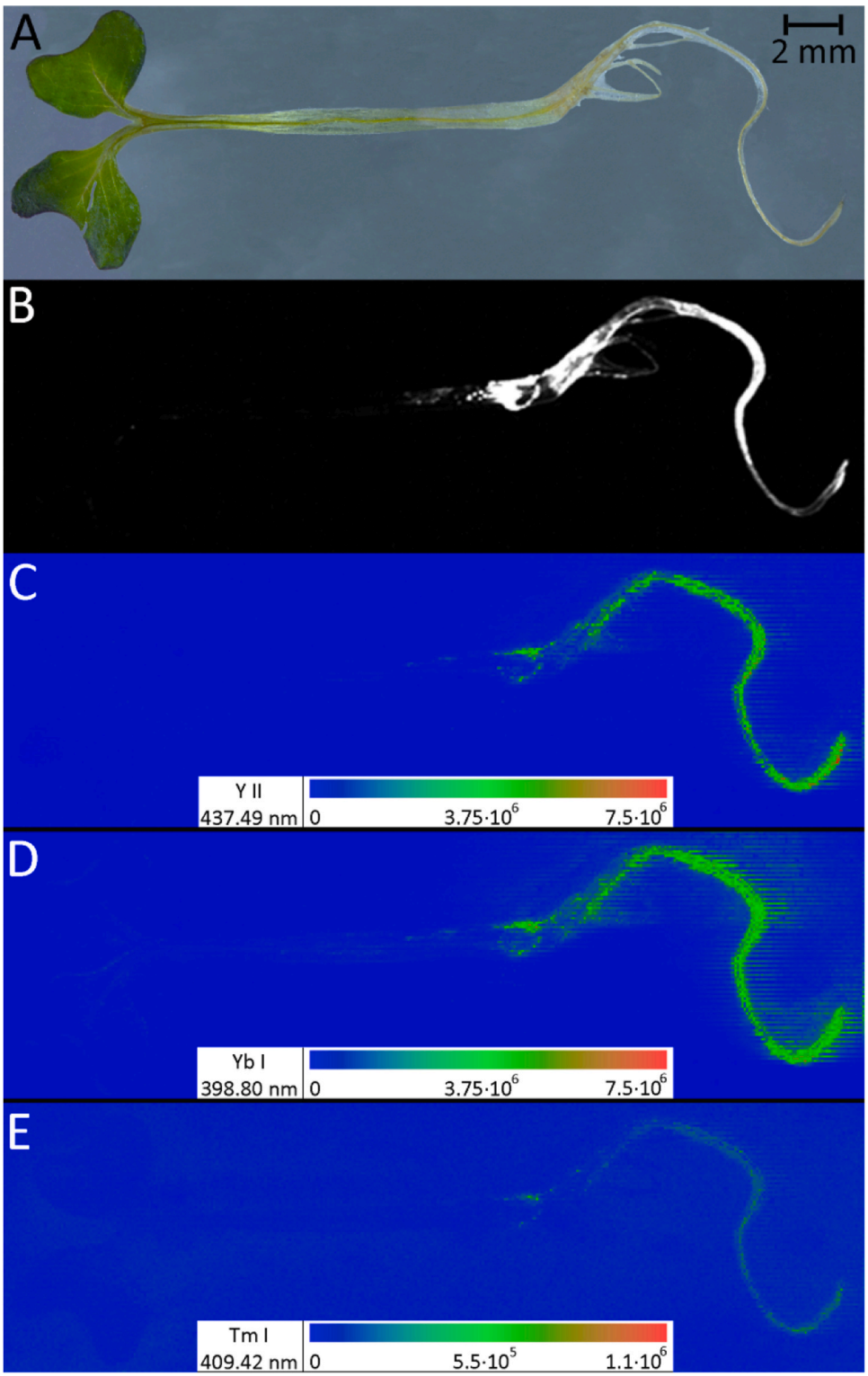

Fig. 6. Brassica oleracea after a 72-h exposure to 50 μg UCNPs/mL dispersion, A: photography of plant, B: photon-upconversion microscan of plant, C: 2D LIBS map of spatial yttrium distribution (Y II 437.49 nm), D: 2D LIBS map of spatial ytterbium distribution (Yb I 398.80 nm), E: 2D LIBS map of spatial thulium distribution (Tm I 409.42 nm). The scales show the intensity of emission lines (counts).

2015), and $NaYF_4$:Yb^{3+},Er^{3+} coated with carboxylated silica shell (Modlitbová et al., 2019). Also, it could be caused by the great stability of tested UCNPs as described in previous chapter.

As it was already proved in literature (Ma et al., 2010), the effects of NPs containing rare-earth elements are not related to free ions that are released from NPs into their surroundings but by NPs themselves. Nevertheless, these NPs have no inert shell on the surface or another type of encapsulation in order to be more stable and consequently improve their stability (Ma et al., 2010). This corresponds to previous phytotoxicity studies with UCNPs (Yin et al., 2015; Modlitbová et al., 2019), and the same behaviour is expected here due to the same silica encapsulation of UCNPs as shown previously (Modlitbová et al., 2019).

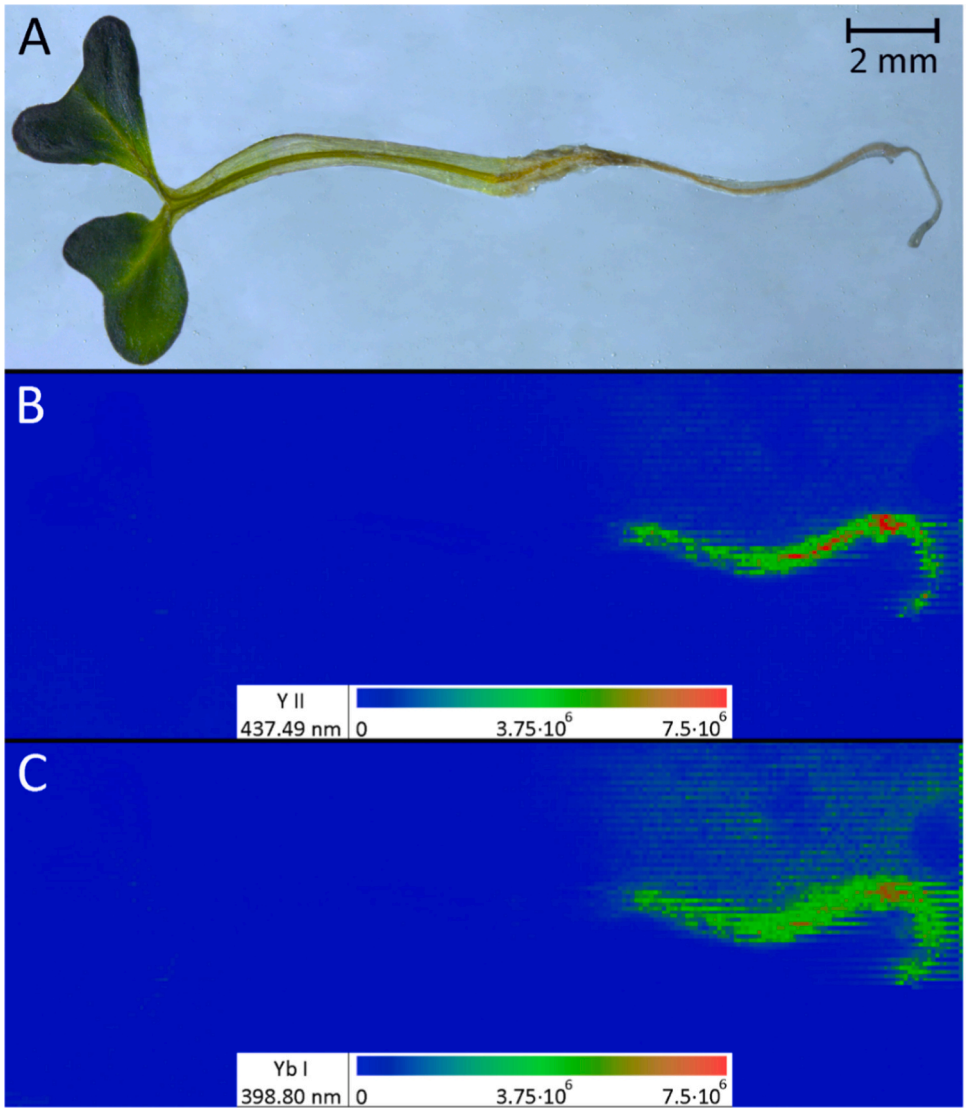

Fig. 7. Brassica oleracea after a 72-h exposure to "50" Y and Yb ions mixture solution, A: photography of plant, B: 2D LIBS map of spatial yttrium distribution (Y II 437.49 nm), C: 2D LIBS map of spatial ytterbium distribution (Yb I 398.80 nm). The scales show the intensity of emission lines (counts).

In accordance with literature, the UCNPs showed a lower toxicity than Y ions (Yin et al., 2015). This situation occurred ordinarily even for other types of NPs (Pokhrel and Dubey, 2013).

3.3. LIBS bioimaging

The emission signals for yttrium (Y II 437.49 nm) and for ytterbium (Yb I 398.80 nm) were accumulated separately after a proper background subtraction using moving minimum for each *B. oleracea* part (root, stem, and leaves). They were normalized to maximum value as shown in the Supplementary data file in Table S3. Then, 2D LIBS maps were constructed for selected elements that UCNPs contained, Y (Y II 437.49 nm), Yb (Yb I 398.80 nm), and Tm (Tm I 409.42 nm). These maps were completed by photon-upconversion microscans to confirm the presence of selected elements in the NPs form. The distribution of elements in *B. oleracea* exposed to 500 μg UCNPs/mL is shown in Fig. 5. The distribution of elements in *B. oleracea* exposed to 50 μg UCNPs/mL is shown in Fig. 6. Also, 2D maps of Y (Y II 437.49 nm) and Yb (Yb I 398.80 nm) were constructed for both positive controls. Fig. 7 shows Y and Yb maps for plant after exposure to "50″ μg/mL ions mixture solution.

The UCNPs were transferred from the root *via* stem into leaves by vascular bundles, which are the main transport corridors for water, inorganic ions, and also for UCNPs (Peng et al., 2012). However, the main bioaccumulation storage organ was the root, which is easily visible on 2D LIBS maps and followingly confirmed also by accumulated signals for Y and Yb as listed in the Table S3. The preference of bioaccumulation sites of UCNPs and ions was as follows. In lower test concentration 50 μg/mL, ions and UCNPs showed the same behaviour in plant translocation, root " stem > leaves, the detected signal from the stem and leaves was negligible. The plants exposed to the 500 μg UCNPs/mL demonstrated different trends. The order of preference was: root > stem " leaves. The same preference of storage organs was present for *R. sativus* exposed to 10 μg UCNPs/mL and to "10″ μg/mL ions mixture solution (Modlitbová et al., 2019). The plants exposed to the "500″ ions solution slightly differed: root > stem = leaves. The trend of bioaccumulation of ions in leaves was shown also for *R. sativus* plants exposed to the ions mixture at a high concentration 1000 μg /mL (Modlitbová et al., 2019). On the contrary, *R. sativus* exposed to 100 a 1000 μg UCNPs/ had a preference in bioaccumulation sites in this order: root > leaves > stem (Modlitbová et al., 2019). This variance might be caused by the different toxicity of UCNPs for plant growth between *R. sativus* and *B. oleracea* plants.

As visible in Figs. 5 and 6, 2D maps of spatial Y, Yb, and Tm

distribution obtained by LIBS method showed a very similar sensitivity in comparison to photon-upconversion microscans. Moreover, LIBS method could easily detect the UCNPs without any luminescence, or UCNPs whose luminescence quench. Also, LIBS offered the bioimaging of selected elements in their ionic forms as showed in the Fig. 7. Thus, LIBS is a robust method for multi-element bioimaging, which is non-dependent on the form of analysed substances.

4. Conclusion

Herein, we report on the toxicity and biodistribution of UCNPs dispersed in aqueous medium for a model crop plant *B. oleracea*. The toxicity was set *via* four macroscopic end-points (root length, stem length, root + stem length, and whole plant length). Based on our findings, we draw several conclusions. (i) The stability of UCNPs in an aquatic dispersion during the exposure, in the direct contact with plant roots, and within test organisms was proved. (ii) The bioaccumulation of rare-earth elements in plants is concentration dependant. (iii) The UCNPs and Y and Yb ions could be transferred from roots through the stem into leaves, however the preferred storage organ is the root. (iv) Tested rare-earth elements are more toxic in ionic forms; actually, UCNPs did not show any toxicity in tested concentrations. (v) The minimal differences in preferences of Y and Yb bioaccumulation sites were observed for the plants exposed to UCNPs or to ions mixtures in the concentration 50 μg/mL. In higher tested concentration 500 μg/mL the change was visible, the UCNPs as well as ions were transferred into leaves *via* stem. In general, it is an extremely challenging task to compile a comprehensive view of UCNPs behaviour in major food crops. Main reasons are the complexity of the problem and the limited information available in the literature. The need of further investigation is apparent.

In this work, we presented LIBS as a fast, straightforward, and quite simple analytical method for semi-quantitative multi-element bioimaging in plant tissues. Also, LIBS enables bioimaging of various NPs after their luminescence quenching and also of NPs without any luminescence, as well as of elements in all other forms. Also, we highlight the possibility of an easy and cheap plant sample preparation with the opportunity for a long-term storage. Finally, LIBS allows the *in-situ* analysis of fresh plants without any sample preparation (Zhao et al., 2016).

CRediT authorship contribution statement

Pavlína Modlitbová conceived and designed the experiments; Sára Střítežská and Antonín Hlaváček performed the experiments; David Prochazka evaluated the LIBS data; Pavlína Modlitbová wrote the original draft; Antonín Hlaváček and Pavel Pořízka edited the draft; Pavel Pořízka and Jozef Kaiser supervised all steps.

Declaration of Competing Interest

The authors declare that they have no known competing financial interests or personal relationships that could have appeared to influence the work reported in this paper.

Acknowledgments

This research has been financially supported by the Ministry of Education, Youth and Sports of the Czech Republic under the project CEITEC 2020 (LQ1601). This work was carried out with the support of grant number FSI-S-20-6353 (Faculty of Mechanical Engineering, Brno University of Technology), CEITEC Nano Research Infrastructure (MEYS CR, 2016-2019), and CEITEC Nano+project, ID CZ.02.1.01/0.0/0.0/16_013/0001728. At the Czech Acad Sci, Inst Anal Chem, the research was supported by the Czech Science Foundation, project no. 18-03367Y and institutional support grant RVO 68081715.

Appendix A. Supporting information

Supplementary data associated with this article can be found in the online version at doi:10.1016/j.ecoenv.2021.112113.

References

Amist, N., Singh, N.B., Yadav, K., Singh, S.C., Pandey, J.K., 2017. Comparative studies of Al^{3+} ions and Al_2O_3 nanoparticles on growth and metabolism of cabbage seedlings. J. Biotechnol. 254, 1–8. https://doi.org/10.1016/j.jbiotec.2017.06.002.

Busser, B., Moncayo, S., Coll, J.L., Sancey, L., Motto-Ros, V., 2018. Elemental imaging using laser-induced breakdown spectroscopy: a new and promising approach for biological and medical applications. Coord. Chem. Rev. 358, 70–79. https://doi.org/10.1016/j.ccr.2017.12.006.

Cui, D., Zhang, P., Ma, Y., He, X., Li, Y., Zhang, J., Zhao, Y., Zhang, Z., 2014. Effect of cerium oxide nanoparticles on asparagus lettuce cultured in an agar medium. Environ. Sci. Nano 1, 459–465. https://doi.org/10.1039/c4en00025k.

Hlaváček, A., Mickert, M.J., Soukka, T., Lahtinen, S., Tallgren, T., Pizúrová, N., Król, A., Gorris, H.H., 2019. Large-scale purification of photon-upconversion nanoparticles by gel electrophoresis for analogue and digital bioassays. Anal. Chem. 91, 1241–1246. https://doi.org/10.1021/acs.analchem.8b04488.

Jantzi, S.C., Motto-Ros, V., Trichard, F., Markushin, Y., Melikechi, N., De Giacomo, A., 2016. Sample treatment and preparation for laser-induced breakdown spectroscopy. Spectrochim. Acta - Part B Spectrosc. 115, 52–63. https://doi.org/10.1016/j.sab.2015.11.002.

Jolivet, L., Leprince, M., Moncayo, S., Sorbier, L., Lienemann, C.-P., Motto-Ros, V., 2019. Review of the recent advances and applications of LIBS-based imaging. Spectrochim. Acta Part B Spectrosc. 151, 41–53. https://doi.org/10.1016/j.sab.2018.11.008.

Ko, J.A., Furuta, N., Lim, H.B., 2019. New approach for mapping and physiological test of silica nanoparticles accumulated in sweet basil (Ocimum basilicum) by LA-ICP-MS. Anal. Chim. Acta 1069, 28–35. https://doi.org/10.1016/j.aca.2019.04.033.

Krajcarová, L., Novotný, K., Kummerová, M., Dubová, J., Gloser, V., Kaiser, J., 2017. Mapping of the spatial distribution of silver nanoparticles in root tissues of Vicia faba by laser-induced breakdown spectroscopy (LIBS). Talanta 173, 28–35. https://doi.org/10.1016/j.talanta.2017.05.055.

Ma, Y., Kuang, L., He, X., Bai, W., Ding, Y., Zhang, Z., Zhao, Y., Chai, Z., 2010. Effects of rare earth oxide nanoparticles on root elongation of plants. Chemosphere 78, 273–279. https://doi.org/10.1016/j.chemosphere.2009.10.050.

Magnuson, B.A., Jonaitis, T.S., Card, J.W., 2011. A brief review of the occurrence, use, and safety of food-related nanomaterials. J. Food Sci. 76, 126–133. https://doi.org/10.1111/j.1750-3841.2011.02170.x.

Modlitbová, P., Hlaváček, A., Švestková, T., Pořízka, P., Šimoníková, L., Novotný, K., Kaiser, J., 2019. The effects of photon-upconversion nanoparticles on the growth of radish and duckweed: bioaccumulation, imaging, and spectroscopic studies. Chemosphere 225, 723–734. https://doi.org/10.1016/j.chemosphere.2019.03.074.

Modlitbová, P., Pořízka, P., Kaiser, J., 2020a. Laser-induced breakdown spectroscopy as a promising tool in the elemental bioimaging of plant tissues. TrAC Trends Anal. Chem. 122, 115729 https://doi.org/10.1016/j.trac.2019.115729.

Modlitbová, P., Pořízka, P., Střítežská, S., Zezulka, Š., Kummerová, M., Novotný, K., Kaiser, J., 2020b. Detail investigation of toxicity, bioaccumulation, and translocation of Cd-based quantum dots and Cd salt in white mustard. Chemosphere 251, 126174. https://doi.org/10.1016/j.chemosphere.2020.126174.

Peng, J., He, Y., Ye, L., Shen, T., Liu, F., Kong, W., Liu, X., Zhao, Y., 2017. Moisture influence reducing method for heavy metals detection in plant materials using laser-induced breakdown spectroscopy: a case study for chromium content detection in rice leaves. Anal. Chem. 89, 7593–7600. https://doi.org/10.1021/acs.analchem.7b01441.

Peng, J., Sun, Y., Liu, Q., Yang, Y., Zhou, J., Feng, W., Zhang, X., Li, F., 2012. Upconversion nanoparticles dramatically promote plant growth without toxicity. Nano Res. 5, 770–782. https://doi.org/10.1007/s12274-012-0261-y.

Pokhrel, L.R., Dubey, B., 2013. Evaluation of developmental responses of two crop plants exposed to silver and zinc oxide nanoparticles. Sci. Total Environ. 452–453, 321–332. https://doi.org/10.1016/j.scitotenv.2013.02.059.

Pořízka, P., Klus, J., Képeš, E., Prochazka, D., Hahn, D.W., Kaiser, J., 2018. On the utilization of principal component analysis in laser-induced breakdown spectroscopy data analysis, a review. Spectrochim. Acta - Part B Spectrosc. 148, 65–82. https://doi.org/10.1016/j.sab.2018.05.030.

Reeves, R.D., Baker, A.J.M., Jaffré, T., Erskine, P.D., Echevarria, G., van der Ent, A., 2018. A global database for plants that hyperaccumulate metal and metalloid trace elements. New Phytol. 218, 407–411. https://doi.org/10.1111/nph.14907.

Rodrigues, S.M., Trindade, T., Duarte, A.C., Pereira, E., Koopmans, G.F., Römkens, P.F.A.M., 2016. A framework to measure the availability of engineered nanoparticles in soils: Trends in soil tests and analytical tools. TrAC - Trends Anal. Chem. 75, 129–140. https://doi.org/10.1016/j.trac.2015.07.003.

Schwabe, F., Tanner, S., Schulin, R., Rotzetter, A., Stark, W., Von Quadt, A., Nowack, B., 2015. Dissolved cerium contributes to uptake of Ce in the presence of differently sized CeO_2-nanoparticles by three crop plants. Metallomics 7, 466–477. https://doi.org/10.1039/c4mt00343h.

Sedlmeier, A., Hlaváček, A., Birner, L., Mickert, M.J., Muhr, V., Hirsch, T., Corstjens, P.L.A.M., Tanke, H.J., Soukka, T., Gorris, H.H., 2016. Highly sensitive laser scanning of photon-upconverting nanoparticles on a macroscopic scale. Anal. Chem. 88, 1835–1841. https://doi.org/10.1021/acs.analchem.5b04147.

Singh, A., Singh, N.B., Hussain, I., Singh, H., 2017. Effect of biologically synthesized copper oxide nanoparticles on metabolism and antioxidant activity to the crop plants

Solanum lycopersicum and Brassica oleracea var. botrytis. J. Biotechnol. 262, 11–27. https://doi.org/10.1016/j.jbiotec.2017.09.016.

Škarková, P., Novotný, K., Lubal, P., Jebavá, A., Pořízka, P., Klus, J., Farka, Z., Hrdlička, A., Kaiser, J., 2017. 2D distribution mapping of quantum dots injected onto filtration paper by laser-induced breakdown spectroscopy. Spectrochim. Acta - Part B Spectrosc. 131, 107–114. https://doi.org/10.1016/j.sab.2017.03.016.

US EPA, 1996. The United States Environmental Protection Agency (US EPA). Ecological Effects Test Guidelines, OPPTS 850.4200, Seed Germination/Root Elongation Toxicity Test. EPA 712-C-96–154, Prevention, Pesticides and Toxic Substances, p. 7170.

Vittori Antisari, L., Carbone, S., Gatti, A., Vianello, G., Nannipieri, P., 2015. Uptake and translocation of metals and nutrients in tomato grown in soil polluted with metal oxide (CeO_2, Fe_3O_4, SnO_2, TiO_2) or metallic (Ag, Co, Ni) engineered nanoparticles. Environ. Sci. Pollut. Res. 22, 1841–1853. https://doi.org/10.1007/s11356-014-3509-0.

Wang, W., Keturi, P.H., 1990. Comparative seed germination tests using ten plant species for toxicity assessment of a metal engraving effluent sample. Water Air Soil Pollut. 52, 369–376. https://doi.org/10.1007/BF00229444.

Wang, Z., Xie, X., Zhao, J., Liu, X., Feng, W., White, J.C., Xing, B., 2012. Xylem- and phloem-based transport of CuO nanoparticles in maize (Zea mays L.). Environ. Sci. Technol. 46, 4434–4441. https://doi.org/10.1021/es204212z.

Yaroshchyk, P., Eberhardt, J.E., 2014. Automatic correction of continuum background in laser-induced breakdown spectroscopy using a model-free algorithm. Spectrochim. Acta - Part B Spectrosc. 99, 138–149. https://doi.org/10.1016/j.sab.2014.06.020.

Yin, W., Zhou, L., Ma, Y., Tian, G., Zhao, J., Yan, L., Zheng, X., Zhang, P., Yu, J., Gu, Z., Zhao, Y., 2015. Phytotoxicity, translocation, and biotransformation of NaYF4 upconversion nanoparticles in a soybean plant. Small 11, 4774–4784. https://doi.org/10.1002/smll.201500701.

Zhao, C., Dong, D., Du, X., Zheng, W., 2016. In-field, in situ, and in vivo 3-dimensional elemental mapping for plant tissue and soil analysis using laser-induced breakdown spectroscopy. Sensors 16, 1764. https://doi.org/10.3390/s16101764.

Zhou, J., Liu, Q., Feng, W., Sun, Y., Li, F., 2015. Upconversion luminescent materials: advances and applications. Chem. Rev. 115, 395–465. https://doi.org/10.1021/cr400478f.